Title

Hot moments drive extreme nitrous oxide and methane emissions from agricultural peatlands

Journal

Global Change Biology, 27(20)

ISSN

1354-1013

Authors

Anthony, Tyler L
Silver, Whendee L

Publication Date

2021-10-01

DOI

10.1111/gcb.15802

Title: Hot moments drive extreme nitrous oxide and methane emissions from agricultural peatlands

Running Head: Drained peatland greenhouse gas emissions

Authors: Tyler L. Anthony[1*], Whendee L. Silver[1]

ORCIDs: MR. TYLER ANTHONY ORCID: 0000-0001-8235-6980
DR. WHENDEE SILVER ORCID: 0000-0003-0372-8745

Affiliations:
[1]Ecosystem Science Division, Department of Environmental Science, Policy and Management, University of California at Berkeley

Contact Info:
*Corresponding author: Tyler L. Anthony, Department of Environmental Science, Policy, and Management, University of California Berkeley, 130 Mulford Hall, Berkeley, CA 94720, USA (t.anthony@berkeley.edu)

Keywords: nitrous oxide, methane, drained peatlands, agricultural peatlands, hot moments, greenhouse gas flux.

Abstract:

Agricultural peatlands are estimated to emit approximately one third of global greenhouse gas emissions from croplands, but the temporal dynamics and controls of these emissions are poorly understood, particularly for nitrous oxide (N_2O). We used cavity ringdown spectroscopy and automated chambers in a drained agricultural peatland to measure over 70,000 individual N_2O, methane (CH_4), and carbon dioxide (CO_2) fluxes over 3 years. Our results showed that N_2O fluxes were high, contributing 26% (annual range: 16-35%) of annual CO_2e emissions. Total N_2O fluxes

This article has been accepted for publication and undergone full peer review but has not been through the copyediting, typesetting, pagination and proofreading process, which may lead to differences between this version and the Version of Record. Please cite this article as doi: 10.1111/GCB.15802

averaged 26 ± 0.5 kg N_2O-N ha^{-1} y^{-1} and exhibited significant inter- and intra-annual variability with a maximum annual flux of 42 ± 1.8 kg N_2O-N ha^{-1} y^{-1}. Hot moments of N_2O and CH_4 emissions represented 1.1 ± 0.2 and 1.3 ± 0.2% of measurements, respectively, but contributed to 45 ± 1% of mean annual N_2O fluxes and to 140 ± 9% of mean annual CH_4 fluxes. Soil moisture, soil temperature, and bulk soil oxygen (O_2) concentrations were strongly correlated with soil N_2O and CH_4 emissions; soil nitrate (NO_3^-) concentrations were also significantly correlated with soil N_2O emissions. These results suggest that IPCC benchmarks underestimate N_2O emissions from these high emitting agricultural peatlands by up to 70%. Scaling to regional agricultural peatlands with similar management suggests these ecosystems could emit up to 1.86 Tg CO_2e y^{-1} (range: 1.58-2.21 Tg CO_2e y^{-1}). Data suggest that these agricultural peatlands are large sources of greenhouse gases, and that short-term hot moments of N_2O and CH_4 are a significant fraction of total greenhouse budgets.

1 | INTRODUCTION

Drained peatlands occupy only 1% of agricultural land but are estimated to emit 32% of global cropland carbon dioxide (CO_2)-equivalent (CO_2e) emissions (Carlson et al., 2017; Leifeld & Menichetti, 2018). As peatland soils are drained and exposed to the atmosphere, high rates of aerobic decomposition lead to substantial CO_2 respiration rates relative to other ecosystems (Hemes et al., 2019; Tiemeyer et al., 2016; Veber et al., 2017). High rates of peat decomposition along with emissions of other important greenhouse gases (GHG) like methane (CH_4) and nitrous oxide (N_2O) can result in large net GHG emissions from these agricultural ecosystems (Oertel, Matschullat, Zurba, Zimmermann, & Erasmi, 2016; Pärn et al., 2018; Petrescu et al., 2015).

Nitrogen fertilization and flood irrigation are common in peatland agriculture (Kirk, Van Kessel, Horwath, & Linquist, 2015; Pellerin, Anderson, & Bergamaschi, 2014; Verhoeven & Setter, 2010), potentially creating optimal conditions for high denitrification rates and N_2O production. Drained peatlands have been shown to be significant N_2O sources; the IPCC mean estimate for drained agricultural peatlands is 8 kg N_2O-N ha^{-1} y^{-1} (uncertainty range: 2-24 kg N_2O-N ha^{-1} y^{-1},

IPCC, 2019). However, few studies have made continuous multi-year measurements of N_2O emissions, and N_2O fluxes are often absent from long-term agricultural peatland GHG budgets (Bonn et al., 2014; Frolking et al., 2011; Günther et al., 2020; Hemes et al., 2019; Knox et al., 2015). This is partially driven by the technological challenges of conducting continuous, long-term N_2O flux measurements under field conditions (Baldocchi, 2014; Levy et al., 2017; Rochette & Eriksen-Hamel, 2008).

Most N_2O flux measurements are conducted intermittently with sampling frequency often ranging from once per day to once per month using traditional manual static chambers (Grace et al., 2020). This is particularly true in agricultural peatlands (H. Liu, Zak, Rezanezhad, & Lennartz, 2019; Pärn et al., 2018; Tiemeyer et al., 2016). However, CH_4 and N_2O are often characterized by hot spots and hot moments of GHG emissions (Krichels & Yang, 2019; Molodovskaya et al., 2012; Savage, Phillips, & Davidson, 2014), which are difficult to characterize using infrequent manual sampling approaches (Bernhardt et al., 2017; McClain et al., 2003; Sihi, Davidson, Savage, & Liang, 2020). The dynamics of soil oxygen (O_2), temperature, moisture, and nitrate (NO_3) concentrations are likely to contribute to hot moments of soil N_2O flux (Butterbach-Bahl, Baggs, Dannenmann, Kiese, & Zechmeister-Boltenstern, 2013), although the spatial and temporal dynamics of these events are also difficult to predict without high frequency measurement.

Potential hot moments of soil CH_4 fluxes are similarly difficult to capture utilizing manual chamber methods, although CH_4 fluxes from drained agricultural peatlands are assumed to be minimal (Günther et al., 2020; Maljanen et al., 2010; Oktarita, Hergoualc'H, Anwar, & Verchot, 2017). However, management practices such as irrigation can create periods of anaerobic conditions ideal for CH_4 production (Hemes et al., 2019; Teh et al., 2011). Continuous eddy covariance measurements of CH_4 fluxes at the ecosystem-scale have highlighted the influence of soil temperature, water table fluctuations, and plant activity on the exchange of CH_4 across the land-atmosphere interface in restored wetlands (Chamberlain et al., 2019; Oikawa et al., 2017; Sturtevant et al., 2016). In contrast, the spatiotemporal controls on the magnitude and frequency of CH_4 fluxes in irrigated agricultural soils are less well constrained.

The recent development of cavity ringdown spectroscopy and automated chamber measurements has greatly increased the ability to conduct continuous GHG flux measurements.

Continuous measurements can increase the chances of capturing hot moments of net GHG fluxes and determining their role in annual GHG budgets. In combination with continuous soil sensor data, spatiotemporally intensive measurements can also be utilized to explore potential drivers of hot moments of soil CH_4 and N_2O emissions (Bernhardt et al., 2017; Groffman et al., 2009; Sihi et al., 2020). We used cavity ringdown spectroscopy and automated chambers to make over 70,000 soil CO_2, CH_4, and N_2O flux measurements over three years from a drained agricultural maize peatland in California, USA. Flux measurements were coupled with continuous soil O_2, temperature, and moisture sensors and a year-long soil N sampling campaign to better constrain the drivers and controls on hot moments of soil CH_4 and N_2O emissions. We utilized multiple statistical approaches, including wavelet coherence analysis and a modified jackknifing technique to further explore the drivers and controls on hot moments of soil CH_4 and N_2O effluxes. We tested the hypothesis that fertilizer application would drive hot moments of N_2O emission through increased substrate availability. We also hypothesized that elevated soil temperatures and soil moisture would stimulate O_2 depletion during the growing season, leading to increased N_2O and CH_4 production within the soil profile and associated hot moments of GHG emissions.

2 | METHODS

2.1 | Site Information

The study was conducted in the Sacramento-San Joaquin Delta region of California (38.11ºN, 121.5ºW). The field site was farmed continuously for over 10 years for conventional field corn (*Zea mays*). The site was periodically irrigated via spud ditches during the growing season and periodically flooded up to 30 cm above the soil surface in the winter to limit weed growth and provide habitat for migrating waterfowl (Pellerin et al. 2014). Fertilizer application rates were 118 kg N ha^{-1} y^{-1} (*Farmer data)*. The climate is Mediterranean with hot dry summers and cool wet winters. The region's historical mean annual temperature was 15.1 ± 6.3 °C and mean annual rainfall averaged 326 ± 4 mm (Hatala et al., 2012). This was also an Ameriflux site (Ameriflux ID: US-Bi2) with continuous eddy covariance measurements of CO_2, CH_4, and water vapor since mid-2017.

Soils are typical of the region and are classified within the Rindge series as Histosols (Soil Survey Staff, 2020). This soil type is frequently drained for agriculture due to its high agricultural

productivity (Leinfelder-Miles, 2019). Rindge soils belong to the Euic, thermic Typic Haplosaprists taxonomic class and are characterized by deep, poorly drained marsh soils formed from decomposed plant organic matter (Soil Survey Staff, 2020). Total soil C values (mean ± standard error) at this site were 15.2 ± 0.4% at 0-15 cm, 15.9 ± 0.7% at 15-30 cm, and 19.5 ± 0.6% at 30-60 cm depth (Anthony & Silver, 2020). Total soil N values were 1.0 ± 0.02% at 0-15 cm, 1.1 ± 0.04% at 15-30 cm, and 1.2 ± 0.03% at 30-60 cm depth (Anthony & Silver, 2020).

2.2 | Automated chamber flux measurements

Surface soil fluxes of N_2O, CH_4, and CO_2 were measured continuously from June 30, 2017 through June 30, 2020 using an automatic chamber system. This system consisted of nine opaque automated gas flux chambers (eosAC, Eosense, Nova Scotia, Canada) connected to a multiplexer (eosMX, Eosense, Nova Scotia, Canada). The multiplexer allowed for dynamically signaled chamber deployment and routed gases to a cavity ring-down spectrometer (Picarro G2508, Santa Clara, CA, USA). Chambers were measured sequentially over a 10-min sampling period with a 1.5-min flushing period before and after each measurement.

Chambers were deployed in 10 x 10 m grid, with each chamber 5 m apart. Due to periodic flooding events, two sets of extended soil collars were utilized to maintain measurement collection and ensure chambers were not inundated. Chambers were randomly assigned to distinct physical features, beds (n = 4) or furrows (n = 5) during growing seasons and corn stover (n = 4) or bare soil (n = 5) during fallow periods. Throughout most of the year, 15 cm collars were installed with each chamber, offsetting the original chamber height by approximately 10 cm. Due to winter flooding events that raise the water table up to 30 cm above the soil surface, additional 35 cm collars were deployed approximately between November and February. Individual chamber volumes were measured and used to adjust flux calculations (see below). Chambers remained installed in their original positions throughout the field campaigns except during field management activities (plowing, seeding, harvest), which typically lasted less than one week. Two additional periods of chamber removal occurred after delays in initiating corn harvest in site year 1 (18 days) and site year 3 (20 days).

To determine chamber volume, collar heights were measured approximately weekly and values were interpolated over time to account for differences in soil and water table height. Chamber volumes were used to calculate the minimum detectable flux (Courtois et al., 2018) with detection limits of 0.002 nmol N_2O m^{-2} s^{-1}, 0.06 nmol CO_2 m^{-2} s^{-1}, and 0.002 nmol CH_4 m^{-2} s^{-1} for 15 cm collars utilized during non-flooded conditions, and 0.004 nmol N_2O m^{-2} s^{-1}, 0.12 nmol CO_2 m^{-2} s^{-1}, and 0.004 nmol CH_4 m^{-2} s^{-1} for 35 cm collars utilized during flooded conditions. The minimum detectable fluxes reported here are conservative estimates, as the actual chamber volume was always smaller than the maximum theoretical volume used in detection limit calculations.

Flux calculations and fitting were first performed using Eosense eosAnalyze-AC v. 3.7.7 software, then data quality assessment and control were subsequently performed in R (RStudio, v.1.1.4633, O'Connell, Ruan, & Silver, 2018). Fluxes were removed from the final dataset if they were associated with negative gas concentrations or erroneous spectrometer cavity temperature and pressure readings outside the calibrated operating range, corresponding to instrument malfunction. Fluxes were also removed if the chamber deployment period was less than 9 min or greater than 11 min, indicative of chamber malfunction. This data filtering removed 2.4% of flux measurement periods, generating a final dataset of 71,262, 70,337, and 70,554 individual flux measurements of CO_2, N_2O, and CH_4, respectively. To calculate the impact of soil GHG fluxes on site-level global warming potential (GWP) we utilized net ecosystem exchange (NEE) eddy covariance values at the same site (Camilo, Szutu, Baldocchi, & Hemes, 2016; Hemes et al., 2019). To convert flux measurements to CO_2e, we used the IPCC AR5 100-year GWP values of 28 CO_2e for CH_4 and 298 CO_2e for N_2O (Myhre et al., 2013). Yield-based emission estimates were from derived flux measurements and harvest yield data records that were converted to g dry yield ha^{-1}, assuming corn was harvested at 65% moisture (Hemes et al., 2019).

2.3 | Quantifying hot moments of CO_2, N_2O, and CH_4

Following data filtering, the importance of very high flux events was determined to identify hot moments and their impact on yearly flux values. We defined hot moments as measurements with values greater than four standard deviations from the mean, as statistically 99.9% of the population should fall within four standard deviations of the mean. Yearly mean flux values were then calculated

for only hot moments, the entire flux dataset, and the flux dataset with not moments removed to determine the impact of very high flux events on annual GHG emissions. The term "outlier" is often used to connote values requiring removal or transformation within a dataset to maintain statistical power and limit overinflated estimates from high leverage observations (Lintott & Mathews, 2018). However, systematic elimination or data transformation ignore or underweight important processes such as hot moments of GHG flux (Benhadi-Marín, 2018; Wiggins, 2000). Given our large and continuous dataset, we could also compare mean fluxes with and without hot moments (Benhadi-Marín, 2018) to better quantify the importance of hot moments. We further explored the importance of capturing hot moments by also recalculating mean N_2O and CH_4 flux after excluding fluxes greater than one, two, and three standard deviations from the mean.

A modified statistical jackknifing technique was used to explore the response of mean N_2O and CH_4 flux estimates to changes in sampling interval by repeatedly sampling the dataset at 1-, 2-, 7-, 14-, and 28-day intervals (Barton et al., 2015). As our flux measurements exhibited a standard normal distribution, the importance of sampling frequency was further explored by calculating the minimum number of random flux measurements (n) needed to accurately recalculate the observed mean N_2O and CH_4 flux values with a 95% confidence interval using equation 1:

$$n \geq \left(\frac{z^* \sigma}{MOE}\right)^2 \quad (1)$$

Where n is minimum sample size, z* is z-score, σ is the standard deviation of the dataset, and MOE is a chosen margin of error (MOE). Using a 95% confidence interval (z score = 1.96), we calculated the minimum number of samples needed for a margin of error of 10%, 25%, and 50% for both annual and total (three year) mean flux values of N_2O and CH_4. Minimum sample size calculations were performed in R with the package samplingbook 1.2.4 (Manitz et al. 2020).

2.4 | Weekly soil measurements

A total of 53 weekly sets of soil samples (n = 10 per week) were collected from the 0-15 cm depth from April 2018 to May 2019. Soil samples were analyzed for gravimetric soil moisture by drying 10 g of field-fresh soil to a constant weight at 105 ˚C, and for soil pH in a slurry of 10 g of field-fresh soil in 10 mL of distilled deionized water (McLean, 1982). Nitrate (NO_3^-) plus nitrite

(NO_2^-) and ammonium (NH_4^+) were measured after extraction of 15 g of field-fresh soil in 75 mL of 2M potassium chloride (KCl) solution (Hart, Stark, Davidson, & Firestone, 1994). Soil KCl extracts were analyzed colorimetrically using an AQ300 analyzer (Seal Instruments, Mequon, WI).

2.5 | Soil sensor measurements

Two sets of soil sensors were installed from September 2018-July 2020 at depths of 10 cm, 30 cm, and 50 cm. Combination SO-110 Oxygen (O_2) and thermistor temperature sensors (Apogee Instruments, Logan, UT) and CS616 moisture sensors (Campbell Scientific, Logan, UT) were connected to CR1000 dataloggers (Campbell Scientific, Logan, UT) that stored data at 15 min intervals. A period of sensor removal occurred in May and June 2019 as multiple agricultural events, including tillage, planting, and discing prevented continuous installation. Sensors were also removed for 3 weeks in September-October 2019 for crop harvest and discing and for 2 weeks the following spring before planting, April to May 2020. Erroneous data corresponding to sensor malfunction were removed from the dataset, which include 0.6% (n = 295) of soil moisture measurements and 0.05% (n = 24) of soil O_2 and temperature measurements. Power loss also contributed to data loss, with a total of 58 days of missing data from agricultural activity or power loss during the sensor measurement period (n = 665 days).

2.6 | Weekly soil gas samples

To explore the potential distribution of GHG production across the soil profile, two replicate soil gas samples (n = 2 per depth per week) for CO_2, CH_4, and N_2O were also taken in parallel with the soil sensors above at 10 cm, 30 cm, and 50 cm depths weekly during unflooded periods from September 2018 through November 2018, and April through December 2019. Instrument grade stainless steel 1/8" tubing (Restek, Bellefonte, PA) was installed in parallel to the soil sensors above, with approximately 15 cm of tubing installed with multiple sampling holes parallel to the soil surface. Sampling septa (Restek, Bellefonte, PA) were installed in 1/8" Swagelok unions (Swagelok Solon, OH) permanently connected to the stainless-steel tubing. Septa were changed monthly. Two gas samples were collected with 30 ml BD syringes, discarding the first sample to clear the dead volume in the sampling line. Sampling lines were removed from the field in May and June 2019 for tillage,

planting, and discing. The 30 ml gas samples were stored in over-pressurized 20 mL glass vials with thick septa (Geomicrobial Technologies, Oechelata, OK) until manual sample injection analysis on a Shimadzu GC-34 (Shimadzu Corp., Tokyo, Japan).

2.7 | Statistical Analyses

Differences in soil gas concentrations, O_2, moisture, mineral N, and pH across time periods were tested with one-way analysis of variance (ANOVA). Growing season time periods were classified as planting date to harvest date, preceded and followed by fallow periods. Unflooded periods were defined as soil moisture less than 50% at 10 cm depth. For CH_4 fluxes, anaerobic periods were defined as any period of time where daily 10 cm O_2 concentrations were equal to 0. Linear regressions were used to explore relationships between soil atmosphere GHG concentrations and net soil GHG fluxes (Figures S2-S4).

2.8 | Wavelet coherence analysis

Wavelet coherence analysis was used to identify interactions between GHG fluxes and the soil variables measured (P. C. Liu, 1994; Wood, Detto, & Silver, 2013). Wavelet-coherence analysis measures the cross-correlation between two time series and allowed us to explore relationships between GHG fluxes and potential controls at daily, monthly, and annual timescales. Wavelet coherence is derived from two time series as a function of decomposed frequency (Wave.xy) and the wavelet power spectrum (Power.x, Power.y) of each individual time series (Rösch & Schmidbauer, 2018):

$$Coherence = \frac{|Wave.xy|^2}{Power.x \cdot Power.y} \quad (2)$$

A more detailed description of the approach and calculations can be found in Rösch & Schmidbauer (2018) and Wood et al., (2013). Missing data were replaced with zeroes to compute an unbiased estimator of the wavelet variance for gappy time series (Mondal & Percival, 2010; Wood et al., 2013). Statistical significance (*p*-value) was computed using 1000 Monte Carlo simulations. All wavelet decomposition and coherence calculations were conducted using the WaveletComp 1.1 package (Rösch & Schmidbauer, 2018) in R (RStudio, v.1.1.4633).

2.9 | Upscaling calculations

We conducted a hypothetical upscaling exercise to estimate the potential impact of agricultural maize peatland emissions in the region. We multiplied our annual GWP values with areal values of 40,000 ha for agricultural maize with similar management practices on peatland soils in the Rindge soil series within the Sacramento-San Joaquin Delta, California, USA (Deverel, Ingrum, & Leighton, 2016; Soil Survey Staff, 2020). Similar management throughout the region includes conventional maize agricultural practices and winter flooding of fallow maize fields to limit weed growth and provide habitat for migrating waterfowl (Central Valley Joint Venture, 2006; Pellerin et al., 2014).

3 | RESULTS

3.1 | Soil CO_2, CH_4 and N_2O emissions

Annual soil GHG emissions averaged 9.20 ± 0.04 CO_2 kg m^{-2} y^{-1}, 4.08 ± 0.10 g N_2O m^{-2} y^{-1} and of 681 ± 157 CH_4 mg m^{-2} y^{-1} (Table 1, Table S1) representing mean annual area- and yield-scaled emissions GWP emissions of 46.7 Mg CO_2e ha^{-1} y^{-1} (range: 39.1-55.5 Mg CO_2e ha^{-1} y^{-1}) and 2.88 kg CO_2e kg dry $yield^{-1}$ y^{-1} (range: 2.41-3.42 kg CO_2e kg dry $yield^{-1}$ y^{-1}), respectively. For N_2O, annual fluxes amount to up to 41.5 ± 1.8 kg N_2O-N ha^{-1} y^{-1} and a mean flux over the three years of 26.0 ± 0.5 kg N_2O-N ha^{-1} y^{-1} or 26% of the GWP (Table 1). We found high intra- and interannual variability in CH_4 fluxes ranging from annual net consumption rates of -111.0 ± 5.0 mg CH_4 m^{-2} y^{-1} to net emissions of 2220.1 ± 519.7 mg CH_4 m^{-2} y^{-1} (Table 1). This corresponded to a maximum annual emission rate of 6.1 ± 1.4 kg CH_4-C ha^{-1} y^{-1}, or 2% of the annual GWP for this ecosystem. Soil respiration was less variable, with annual values ranging from 6.61 ± 0.07 kg CO_2 m^{-2} y^{-1} to 10.72 ± 0.09 kg CO_2 m^{-2} y^{-1} (Figure 1a, Table S1).

3.2 | Quantifying hot moments of soil CO_2, CH_4 and N_2O emissions

We defined hot moments conservatively as individual flux measurements that were more than four standard deviations from the yearly mean (Table 1). Hot moment fluxes of N_2O represented only 0.64% to 1.50% of annual measurements but increased the mean flux rate by 38.5% to 76.3% (Table 1). For CH_4, hot moment fluxes were only 0.06% to 0.8% of yearly measurements but increased

yearly mean fluxes by 132.1% to 486.4% in site years two and three. In site year one, hot moments of CH_4 consumption increased the net CH_4 sink by 249.2%. The substantial hot moment driven changes in CH_4 fluxes were largely due to the majority of CH_4 flux measurements recorded at or near zero (Figure 1b). Hot moments of CO_2 emissions had a significantly lower overall impact on mean CO_2 fluxes, representing only 0.5% of all fluxes (annual range 0.3-0.6%). This increased overall mean fluxes by 5% and annual mean CO_2 fluxes by 2.6 to 9.2% (Table S1).

3.3 | Drivers of N_2O fluxes

The onset of winter flooding increased soil N_2O emissions exponentially, with daily average fluxes of up to 395.6 ± 87.6 mg N_2O m^{-2} d^{-1} ($p < 0.001$). Irrigation and fertilizer application during the growing season also significantly increased N_2O fluxes (Figure 2a, $p < 0.001$). We used arrays of soil moisture, temperature, and O_2 sensors and weekly soil gas and mineral nitrogen (N) measurements in combination with continuous surface flux measurements to explore potential controls on GHG fluxes. Daily mean N_2O fluxes increased up to two orders of magnitude shortly after the onset of winter flooding concurrent with a rise in soil moisture and a corresponding reduction in soil O_2 concentrations across soil depths (Figure 2d, $p < 0.001$). Continued inundation led to a decline in soil NO_3^-concentrations (Figure 2b, $p < 0.001$) and a subsequent drop in N_2O fluxes (Figure 2a, $p < 0.001$). Soil gas concentrations were taken at 10 cm, 30 cm, and 50 cm depths during non-flooded periods from September 2018-December 2019. We found that daily mean N_2O fluxes were significantly correlated with soil N_2O concentrations across all depths ($R^2 = 0.45$-0.60, Figure S1), and likely contributed to net fluxes across the soil-atmosphere interface.

Wavelet coherence analysis suggested temporal patterns in soil moisture, soil temperature, and bulk soil O_2 concentrations across all depths were significantly related to patterns in net N_2O fluxes on a daily timescale (Figure S5, $p < 0.05$). Net N_2O fluxes showed significant coherence with soil O_2 concentrations across depths at the seasonal timescale of approximately 100 days, and soil moisture at the yearly scale of approximately 300 days (Figure S5, $p < 0.05$).

3.4 | Drivers of CH_4 and CO_2 fluxes

Significant CH_4 fluxes were only observed 60 days into an extended period of anoxic conditions lasting a total of 124 days. This period of anoxic conditions was associated with complete soil saturation following winter flooding (Figure 3c) and corresponded to decreased soil O_2 concentrations across depths (Figure 3d). Short periods of elevated NH_4^+ concentrations observed during flooding were also associated with decreases in CH_4 production (Figure 3a and 3b). Shorter periods of sustained anoxic conditions in 2019-2020 (50 total days) did not produce hot moments of CH_4 fluxes. Wavelet coherence analysis of CH_4 fluxes suggested that soil moisture, soil temperature, and bulk soil O_2 concentrations drove patterns in net CH_4 fluxes at a daily time scale (Figure S5, $p < 0.05$). Only soil O_2 concentrations across soil depths had significant coherence with CH_4 fluxes on a weekly timescale (Figure S5, $p < 0.05$), with no significant coherence at longer timescales.

Seasonality explained the high intra-annual variation observed in CO_2 fluxes. Higher soil respiration rates (mean 50.5 ± 1.5 g CO_2 m^{-2} d^{-1}) occurred during the growing season and following harvest (July-September). Fluxes were significantly lower (6.8 ± 0.1 g CO_2 m^{-2} d^{-1}) when soils were saturated (December-March). There was significant coherence with moisture, temperature, and O_2 concentrations across depths at the daily scale (Figure S6, $p < 0.05$). At weekly and seasonal scales, temperature and O_2 concentrations displayed significant ($p < 0.05$) coherence with soil CO_2 fluxes. We compared chamber fluxes with ecosystem respiration (R_{eco}) measurements conducted via eddy covariance in parallel at this field site (Camilo et al., 2016; Hemes et al., 2019). Similar values were observed for soil CO_2 chamber fluxes (9.20 ± 0.04 kg CO_2 m^{-2} y^{-1}) and R_{eco} eddy-covariance measurements (9.70 ± 0.01 kg CO_2 m^{-2} y^{-1}) across the study period (Figure S6). Soil CH_4 chamber fluxes (1.2 ± 0.01 g CH_4 m^{-2} y^{-1}) were lower than the eddy-covariance CH_4 fluxes (2.2 ± 0.01 g CH_4 m^{-2} y^{-1}), although eddy covariance also captured similar hot moments of CH_4 emission (Figure S7).

3.5 | Sampling frequency effects on N_2O and CH_4 flux estimates

Decreasing the measurement sampling interval led to significant under- or overestimates of total N_2O and CH_4 flux. Simulating a 28-day (once monthly) sampling interval underestimated total N_2O flux by a median of -13.0% (Range of 28-day N_2O subsets: -75.1% to +129.2%, Table S2) and CH_4 flux by a median of -17.4% (Range of 28-day CH_4 subsets: -88.6 to + 656%, Table S3). A weekly sampling interval underestimated the total N_2O flux by a median of -2.3% (Range of weekly

subsets: -18.3% to +18.8%, Table S2) and total CH_4 flux by a median of +14.1% (Range of 7-day CH_4 subsets: -40.3% to 149% Table S3). A sampling interval of every other day under- or overestimated total N_2O fluxes by ±2.4% but overestimated CH_4 fluxes by +32.9% to +64.4% (Table S2 and 3).

We further explored the importance of missing potential hot moment fluxes by calculating the change in mean N_2O and CH_4 fluxes after removing observations greater than one, two, or three standard deviations from the overall mean flux. Removing all observations more than one standard deviation of the mean underestimated annual N_2O fluxes by 56.6%, while removing observations greater than two and three standard deviations underestimated N_2O fluxes by 42.7% and 34.5%, respectively. Missing N_2O fluxes greater than three standard deviations corresponded to an underestimation of annual N_2O emissions up to 14.3 ± 0.6 kg N-N_2O ha^{-1} yr^{-1}. For CH_4, removing observations greater than one standard deviation underestimated annual CH_4 fluxes by 79%, while removing observations greater than two and three standard deviations underestimated CH_4 fluxes by 69% and 63%, respectively.

Finally, we calculated the minimum number of randomized flux measurements needed to calculate annual and total (3-year) flux values for N_2O and CH_4 with a 95% confidence interval and margins of error of 10%, 25%, and 50% when the occurrence of hot moments are unknown (Table S4). For N_2O, an average of 8,342 (range: 2,700-8,342) individual flux measurements were needed to accurately calculate the annual mean flux within a 10% margin of error. This represents up to 35% (range: 11-35%) of the dataset. Increasing the margin of error to 25% and 50% reduced the number of measurements needed, with a range of 475 to 1,904 and 121 to 507 individual randomized measurements per year, respectively. When analyzing the total N_2O dataset, the minimum number of flux measurements needed was 6,401 with a 10% of margin error, decreasing to 1,108 and 281 for margins of error of 25% and 50%, respectively.

The minimum sample size needed for calculating annual and total mean CH_4 fluxes were greater than N_2O (Table S4). For annual CH_4 fluxes, the minimum sample size needed to recalculate the mean flux within a 10% margin of error was at least 17,133 (range: 17,133-22,525). Increasing the margin of error to 25% and 50% reduced the minimum annual sample sizes needed to at least 7,562 (range: 7,562-18,284) and 2,525 (range: 2,525-10,770), respectively. The minimum number of flux

measurements needed for the total CH_4 dataset was also higher than N_2O with 68,137, 54,419, and 31,656 for margins of error of 10%, 25%, and 50%, respectively.

3.6 | Upscaling greenhouse gas emissions

We conducted an upscaling exercise to provide a first approximation of the potential impact of peatland maize agriculture on regional GHG emissions. Using the three years of field data, we upscaled these flux measurements using the total regional land area with similar soil series and management practices. We calculated a mean annual GWP of 1.86 Tg CO_2e y^{-1} (range: 1.58-2.21 Tg CO_2e y^{-1}) for agricultural peatlands in the region, with N_2O emissions representing 0.48 Tg CO_2e y^{-1} (range: 0.28-0.77 Tg CO_2e y^{-1}). Assuming the field estimates measured here are representative of local management practices, N_2O fluxes alone could represent 26% (annual range: 18-33%) of agricultural maize peatland CO_2e emissions in this region, a significantly higher percentage than previous estimates (Deverel, Jacobs, Lucero, Dore, & Kelsey, 2017; Hemes et al., 2019). Soil types with similar organic matter content represent over 40,000 ha of agricultural peatlands in the Sacramento-San Joaquin Delta region (Deverel et al., 2016; Soil Survey Staff, 2020) and these soils are dominated by maize production. They are often flooded in the winter for waterfowl habitat (Delta Protection Commission, 2012; Pellerin et al., 2014).

4 | DISCUSSION

4.1 | Annual fluxes and hot moments of N_2O emissions

The agricultural peatland soils in this study were extreme N_2O emitters, with mean rates that were 4-27 times greater than other non-peat cropland N_2O emissions (Ferrari Machado et al., 2020; IPCC, 2013; Jin et al., 2014; Johnson, Weyers, Archer, & Barbour, 2012). It is notable that these values for both peatland and non-peatland ecosystems were largely derived from non-continuous data that may not capture all N_2O emission hot moments. The three year average N_2O emissions were greater than the highest IPCC estimates for temperate organic cropland soils, and the peak annual N_2O emissions from this study were five times greater than the average values of 8 kg N_2O-N ha^{-1} y^{-1} (uncertainty range: 2-24 kg N_2O-N ha^{-1} y^{-1}, IPCC, 2019). Estimated mean annual N_2O emissions of

16.8 ± 14.8 kg N_2O-N ha^{-1} y^{-1} have been reported for other drained peatlands with data derived from bulk densities (H. Liu, Wrage-Mönnig, & Lennartz, 2020). Average N_2O emissions observed in this study were similar to or higher than studies of N_2O emissions from agricultural peatlands in the Sacramento-Delta, which ranged from 6.6 ± 3.8 using model estimates (Deverel et al., 2017) to 24 ± 13 kg N_2O-N ha^{-1} y^{-1} using shorter-term periodic manual static chamber measurements (Teh et al., 2011).

Surprisingly winter flooding, not fertilization, was the dominant driver of N_2O emissions. Peak N_2O emissions were observed shortly following winter flooding. The high NO_3^- measured shortly after flooding likely accumulated under oxic, well-drained soil conditions as a result of N mineralization following crop harvest (Kirk et al., 2015), and may have been supplemented by iron coupled anaerobic ammonium oxidation in these iron and C-rich soils (Anthony & Silver, 2020; Golovchenko, Tikhonova, & Zvyagintsev, 2007; Martikainen, Nykänen, Crill, & Silvola, 1993; Yang & Liptzin, 2015; Yang, Weber, & Silver, 2012). Urea-ammonium-nitrate (UAN) fertilizer was applied once per year during planting. This inorganic N fertilizer application also contributed to a short-term increase in N_2O emissions, although this was not the dominant source of annual N_2O emissions.

Denitrification was likely the main pathway of N_2O during hot moments of N_2O flux given elevated NO_3^- concentrations observed immediately prior to peak emissions, as well as the observed increases in soil moisture and decreases in soil O_2 and NO_3^- concentrations during the N_2O hot moments. The NO_3^- was likely consumed during denitrification, with significant amounts of N_2O released as a byproduct of incomplete denitrification in these N-rich soils (Firestone & Davidson, 1989). The strong correlations observed between daily mean N_2O fluxes and soil atmosphere N_2O concentrations also suggest that significant N_2O production was occurring at depth and thus production throughout the profile likely contributed to the large fluxes observed.

4.2 | Fluxes of CH_4 and CO_2

Prolonged anaerobic conditions coupled with soil temperatures greater than 10º C appeared to drive hot moments of CH_4 fluxes in these systems. Short periods of elevated NH_4^+ concentrations during flooded periods could have limited methanogenesis (Chen, Cheng, & Creamer, 2008) or

temporarily shifted the methanogenic pathway (Fotidis, Karakashev, Kotsopoulos, Martzopoulos, & Angelidaki, 2013) and likely contributed to the considerable variability observed. Expectedly, patterns in soil CO_2 fluxes were related to temperature and O_2 concentrations at weekly and seasonal scales. Soil temperature and O_2 availability are important controls on aerobic soil respiration (Kasimir-Klemedtsson et al., 1997), particularly in ecosystems such as drained agricultural peatlands where substrate availability is not likely to be limiting to heterotrophs and nutrient availability to autotrophs is high.

4.3 | The role of hot moments in N_2O and CH_4 fluxes

The large continuous data set allowed us to explore the importance of hot moments of N_2O and CH_4 emission in total ecosystem GHG budgets. While hot moments represented only 0.63-1.50% and 0.06-0.76% of annual N_2O and CH_4 flux measurements, respectively, they contributed up to 76% of total N_2O emissions and 486% of total CH_4 emissions. This corresponded to N_2O hot moment emissions alone contributing up to 18% of the annual GWP of these agricultural peatlands. This highlights that missing hot moments may lead to significant underestimates of total ecosystem GHG budgets.

We also explored the effects of sampling interval on N_2O and CH_4 flux quantification. Our results further highlighted the necessity of continuous measurements to accurately estimate total ecosystem N_2O and CH_4 fluxes. Even weekly sampling intervals may underestimate annual N_2O fluxes by up to 20%, a significant fraction of total GWP, even from these high emitting agricultural peatlands. While continuous automated chamber or eddy covariance measurements are ideal to capture hot moments of emissions, long-term continuous measurements are still cost prohibitive in many locations and ecosystems. If hot moments are predictable and well defined, daily flux measurements are likely effective in appropriately quantifying hot moments of N_2O emissions (Ferrari Machado, Wagner-Riddle, MacTavish, Voroney, & Bruulsema, 2019; Reeves, Wang, Salter, & Halpin, 2016). However if the timing and controls on hot moments are unknown or sporadic, less frequent sampling may significantly underestimate N_2O emissions (Grace et al., 2020). Our results suggest that roughly 8,000 randomized individual chamber flux measurements would be needed to accurately estimate annual N_2O budgets from these agricultural peatlands with a 95% confidence

interval and 10% margin of error, assuming the drivers of hot moments were not well understood. Approximately 500 individual measurements would yield a 50% margin of error. Given the more sporadic nature of CH_4 hot moments, our results suggest that it is even more difficult to accurately estimate CH_4 fluxes with periodic sampling in these ecosystems. Analyses found that at least 17,000 and 2,500 individual flux measurements would be needed to estimate annual CH_4 budgets within a 10% and 50% margin of error, respectively.

4.4 | GHG budgets and upscaling

The agricultural maize peatland soil studied here was a much larger source of soil GHG emissions than other maize agroecosystems. While agricultural peat soils are highly productive, average annual GHG emissions were 3.6-33.3 times greater on an area-scaled basis and 3-15.6 times greater on yield-scaled basis relative to other agricultural maize emissions estimates (Table S5, Chai et al., 2019; Jin et al., 2014; Johnson, Weyers, Archer, & Barbour, 2012; Linquist et al., 2012).

We conducted an upscaling exercise as a first approximation of the potential impacts of maize peatland fluxes on regional GHG budgets. Our estimates suggested that maize agriculture on similar peat soils in the region could emit an average of 1.86 Tg CO_2e y^{-1}. Nitrous oxide emissions alone accounted for approximately 26% of the total. This value is significantly higher than previous estimates for the region (Deverel et al., 2017; Hemes et al., 2019) and highlights the importance of including high frequency N_2O measurements to capture hot moments in N_2O fluxes, the disproportionate impact N_2O emissions have on agricultural peatland GHG budgets, and that these agricultural peatlands are significant N_2O sources. We also found that irrigation timing and duration, not fertilization, was the predominant driver of N_2O and CH_4 emissions and a significant source of the total GHG budget. Determining management strategies that reduce soil N_2O and CH_4 emissions, particularly changes in flood irrigation timing and duration, could have a disproportionate impact on reducing total agricultural peatland GHG emissions (Hemes et al., 2019; Knox et al., 2015; McNicol et al., 2017; Windham-Myers et al., 2018).

5 | CONCLUSION

This study presents one of the largest, longest, and most comprehensive soil flux datasets from agricultural peatlands to date. Our results provide evidence that these systems are a significant contributor to agricultural GHG emissions. The continuous dataset allowed us to explore the importance of hot moments of soil CH_4 and N_2O emissions driven by land management changes in soil moisture, soil O_2, and soil N availability. We found that irrigation timing and duration, not fertilization, was the predominant control on soil N_2O and CH_4 emissions from these agricultural peatlands. We also found that N_2O and CH_4 alone contributed up to 37% of the annual GWP of this system. This suggests that land management strategies that limit flooding frequency and duration may significantly reduce total agricultural peatland GHG emissions. We further demonstrate that continuous automated chamber measurements of soil GHG emissions capture hot moments of N_2O and CH_4 production and intensive sampling, particularly during hot moments of emission, are needed to accurately quantify GHG budgets. This is particularly important in high emitting ecosystems such as agricultural peatlands to ensure effective and targeted land management strategies that maximally limit net ecosystem GHG emissions.

6 | ACKNOWLEDGEMENTS

We appreciate assistance from Heather Dang, Tibisay Peréz, and numerous other members of both the Silver Lab and the Berkeley Biometeorology Lab at University of California, Berkeley. We thank Christine O'Connell for the initial code development for data filtering. This work was supported by a Contract by the California Department of Water Resources (award 4600011240). We thank the California Department of Water Resources and the Metropolitan Water District of Southern California for research site access. T. L. Anthony was supported by the California Sea Grant Delta Science Fellowship. This material is based upon work supported by the Delta Stewardship Council Delta Science Program under Grant No. 5298 and California Sea Grant College Program Project R/SF-89. The contents of this material do not necessarily reflect the views and policies of the Delta Stewardship Council or California Sea Grant, nor does mention of trade names or commercial products constitute endorsement or recommendation for use. McIntire Stennis grant CA-B-ECO-7673-MS to W. L. Silver partially supported this work. W. L. Silver was also supported by funds from

Breakthrough Strategies & Solutions, and the V. Kann Rasmussen, Oak Creek, Jewish Community, Northern Trust, and Trisons Foundations. The authors declare no conflict of interests.

7 | DATA AVAILABILITY STATEMENT

The data that support the findings of this study are available from the corresponding author upon reasonable request.

8 | REFERENCES

Anthony, T. L., & Silver, W. L. (2020). Mineralogical associations with soil carbon in managed wetland soils. *Global Change Biology*, (March), 1–13. https://doi.org/10.1111/gcb.15309

Baldocchi, D. (2014). Measuring fluxes of trace gases and energy between ecosystems and the atmosphere - the state and future of the eddy covariance method. *Global Change Biology*, *20*(12), 3600–3609. https://doi.org/10.1111/gcb.12649

Barton, L., Wolf, B., Rowlings, D., Scheer, C., Kiese, R., Grace, P., … Butterbach-Bahl, K. (2015). Sampling frequency affects estimates of annual nitrous oxide fluxes. *Scientific Reports*, *5*, 1–9. https://doi.org/10.1038/srep15912

Benhadi-Marín, J. (2018). A conceptual framework to deal with outliers in ecology. *Biodiversity and Conservation*, *27*(12), 3295–3300. https://doi.org/10.1007/s10531-018-1602-2

Bernhardt, E. S., Blaszczak, J. R., Ficken, C. D., Fork, M. L., Kaiser, K. E., & Seybold, E. C. (2017). Control Points in Ecosystems: Moving Beyond the Hot Spot Hot Moment Concept. *Ecosystems*, *20*(4), 665–682. https://doi.org/10.1007/s10021-016-0103-y

Bonn, A., Reed, M. S., Evans, C. D., Joosten, H., Bain, C., Farmer, J., … Birnie, D. (2014). Investing in nature: Developing ecosystem service markets for peatland restoration. *Ecosystem Services*, *9*, 54–65. https://doi.org/10.1016/j.ecoser.2014.06.011

Butterbach-Bahl, K., Baggs, E. M., Dannenmann, M., Kiese, R., & Zechmeister-Boltenstern, S. (2013). Nitrous oxide emissions from soils: how well do we understand the processes and their controls? *Philosophical Transactions of the Royal Society of London. Series B, Biological Sciences*, *368*(1621), 20130122. https://doi.org/10.1098/rstb.2013.0122

Camilo, R.-S., Szutu, D., Baldocchi, D., & Hemes, K. (2016). AmeriFlux US-Bi2 Bouldin Island

corn. United States. https://doi.org/10.17190/AMF/1419513

Carlson, K. M., Gerber, J. S., Mueller, N. D., Herrero, M., MacDonald, G. K., Brauman, K. A., … West, P. C. (2017). Greenhouse gas emissions intensity of global croplands. *Nature Climate Change*, *7*(1), 63–68. https://doi.org/10.1038/nclimate3158

Central Valley Joint Venture. (2006). Central Valley Joint Venture Implementation Plan 2006, 1–261.

Chai, R., Ye, X., Ma, C., Wang, Q., Tu, R., Zhang, L., & Gao, H. (2019). Greenhouse gas emissions from synthetic nitrogen manufacture and fertilization for main upland crops in China. *Carbon Balance and Management*, *14*(1), 1–10. https://doi.org/10.1186/s13021-019-0133-9

Chamberlain, S. D., Hemes, K. S., Eichelmann, E., Szutu, D. J., Verfaillie, J. G., & Baldocchi, D. D. (2019). Effect of Drought-Induced Salinization on Wetland Methane Emissions, Gross Ecosystem Productivity, and Their Interactions. *Ecosystems*. https://doi.org/10.1007/s10021-019-00430-5

Chen, Y., Cheng, J. J., & Creamer, K. S. (2008). Inhibition of anaerobic digestion process: A review. *Bioresource Technology*, *99*(10), 4044–4064. https://doi.org/10.1016/j.biortech.2007.01.057

Courtois, E. A., Stahl, C., Burban, B., Van den Berge, J., Berveiller, D., Bréchet, L., … Janssens, I. A. (2018). Automatic high-frequency measurements of full soil greenhouse gas fluxes in a tropical forest. *Biogeosciences Discussions*, 1–21. https://doi.org/10.5194/bg-2018-341

Delta Protection Commission. (2012). Economic Sustainability Plan for the Sacramento-San Joaquin Delta. Retrieved from http://www.delta.ca.gov/res/docs/ESP/ESP_P2_FINAL.pdf

Deverel, S. J., Ingrum, T., & Leighton, D. (2016). Present-day oxidative subsidence of organic soils and mitigation in the Sacramento-San Joaquin Delta, California, USA. *Hydrogeology Journal*, *24*(3), 569–586. https://doi.org/10.1007/s10040-016-1391-1

Deverel, S. J., Jacobs, P., Lucero, C., Dore, S., & Kelsey, T. R. (2017). Implications for Greenhouse Gas Emission reductions and economics of a changing agricultural mosaic in the Sacramento - San Joaquin Delta. *San Francisco Estuary and Watershed Science*, *15*(3). https://doi.org/10.15447/sfews.2017v15iss3art2

Ferrari Machado, P. V., Neufeld, K., Brown, S. E., Voroney, P. R., Bruulsema, T. W., & Wagner-Riddle, C. (2020). High temporal resolution nitrous oxide fluxes from corn (Zea mays L.) in response to the combined use of nitrification and urease inhibitors. *Agriculture, Ecosystems and*

Environment, *300*(May), 106996. https://doi.org/10.1016/j.agee.2020.106996

Ferrari Machado, P. V., Wagner-Riddle, C., MacTavish, R., Voroney, P. R., & Bruulsema, T. W. (2019). Diurnal Variation and Sampling Frequency Effects on Nitrous Oxide Emissions Following Nitrogen Fertilization and Spring-Thaw Events. *Soil Science Society of America Journal*, *83*(3), 743–750. https://doi.org/10.2136/sssaj2018.10.0365

Firestone, M. K., & Davidson, E. A. (1989). Microbiologial Basis of NO and N20 production and consumption in soil. *Exchange of Trace Gases between Terrestrial Ecosystems and the Atmosphere*, (January 1989), 7–21.

Fotidis, I. A., Karakashev, D., Kotsopoulos, T. A., Martzopoulos, G. G., & Angelidaki, I. (2013). Effect of ammonium and acetate on methanogenic pathway and methanogenic community composition. *FEMS Microbiology Ecology*, *83*(1), 38–48. https://doi.org/10.1111/j.1574-6941.2012.01456.x

Frolking, S., Talbot, J., Jones, M. C., Treat, C. C., Kauffman, J. B., Tuittila, E. S., & Roulet, N. (2011). Peatlands in the Earth's 21st century climate system. *Environmental Reviews*, *19*(1), 371–396. https://doi.org/10.1139/a11-014

Golovchenko, A. V., Tikhonova, E. Y., & Zvyagintsev, D. G. (2007). Abundance, biomass, structure, and activity of the microbial complexes of minerotrophic and ombrotrophic peatlands. *Microbiology*, *76*(5), 630–637. https://doi.org/10.1134/S0026261707050177

Grace, P. R., van der Weerden, T. J., Rowlings, D. W., Scheer, C., Brunk, C., Kiese, R., … Skiba, U. M. (2020). Global Research Alliance N2O chamber methodology guidelines: Considerations for automated flux measurement. *Journal of Environmental Quality*, *49*(5), 1126–1140. https://doi.org/10.1002/jeq2.20124

Groffman, P. M., Butterbach-Bahl, K., Fulweiler, R. W., Gold, A. J., Morse, J. L., Stander, E. K., … Vidon, P. (2009). Challenges to incorporating spatially and temporally explicit phenomena (hotspots and hot moments) in denitrification models. *Biogeochemistry*, *93*(1–2), 49–77. https://doi.org/10.1007/s10533-008-9277-5

Günther, A., Barthelmes, A., Huth, V., Joosten, H., Jurasinski, G., Koebsch, F., & Couwenberg, J. (2020). Prompt rewetting of drained peatlands reduces climate warming despite methane emissions. *Nature Communications*, *11*(1), 1–5. https://doi.org/10.1038/s41467-020-15499-z

Hart, S. C., Stark, J. M., Davidson, E. A., & Firestone, M. K. (1994). Nitrogen Mineralization, Immobilization, and Nitrification. In R. W. Weaver, J. S. Angle, & P. S. Bottomley (Eds.), *Methods of Soil Analysis, Part 2. Microbial and Biochemical Properties* (pp. 985–1018). Madison, WI: Soil Science Society of America.

Hatala, J. A., Detto, M., Sonnentag, O., Deverel, S. J., Verfaillie, J., & Baldocchi, D. D. (2012). Greenhouse gas (CO2, CH4, H2O) fluxes from drained and flooded agricultural peatlands in the Sacramento-San Joaquin Delta. *Agriculture, Ecosystems and Environment*, *150*, 1–18. https://doi.org/10.1016/j.agee.2012.01.009

Hemes, K. S., Chamberlain, S. D., Eichelmann, E., Anthony, T., Valach, A., Kasak, K., … Baldocchi, D. D. (2019). Assessing the carbon and climate benefit of restoring degraded agricultural peat soils to managed wetlands. *Agricultural and Forest Meteorology*, *268*, 202–214. https://doi.org/10.1016/j.agrformet.2019.01.017

IPCC. (2019). N2O Emissions From Managed Soils, and CO2 Emissions From Lime and Urea Application. *2019 Refinement to the 2006 IPCC Guidelines for National Greenhouse Gas Inventories*, 1–48.

IPCC, 2014. (2013). 2013 Supplement to the 2006 IPCC Guidelines for National Greenhouse Gas Inventories: Wetlands, Hiraishi, T., Krug, T., Tanabe, K., Srivastava, N., Baasansuren, J., Fukuda, M. and Troxler, T.G. (eds).

Jin, V. L., Baker, J. M., Johnson, J. M. F., Karlen, D. L., Lehman, R. M., Osborne, S. L., … Wienhold, B. J. (2014). Soil Greenhouse Gas Emissions in Response to Corn Stover Removal and Tillage Management Across the US Corn Belt. *Bioenergy Research*, *7*(2), 517–527. https://doi.org/10.1007/s12155-014-9421-0

Johnson, J. M. F., Weyers, S. L., Archer, D. W., & Barbour, N. W. (2012). Nitrous Oxide, Methane Emission, and Yield-Scaled Emission from Organically and Conventionally Managed Systems. *Soil Science Society of America Journal*, *76*(4), 1347–1357. https://doi.org/10.2136/sssaj2012.0017

Kasimir-Klemedtsson, Å., Klemedtsson, L., Berglund, K., Martikainen, P., Silvola, J., & Oenema, O. (1997). Greenhouse gas emissions from farmed organic soils: A review. *Soil Use and Management*, *13*(4 SUPPL.), 245–250. https://doi.org/10.1111/j.1475-2743.1997.tb00595.x

Kirk, E. R., Van Kessel, C., Horwath, W. R., & Linquist, B. A. (2015). Estimating annual soil carbon loss in agricultural peatland soils using a nitrogen budget approach. *PLoS ONE*, *10*(3), 1–18. https://doi.org/10.1371/journal.pone.0121432

Knox, S. H., Sturtevant, C., Matthes, J. H., Koteen, L., Verfaillie, J., & Baldocchi, D. (2015). Agricultural peatland restoration: Effects of land-use change on greenhouse gas (CO2 and CH4) fluxes in the Sacramento-San Joaquin Delta. *Global Change Biology*, *21*(2), 750–765. https://doi.org/10.1111/gcb.12745

Krichels, A. H., & Yang, W. H. (2019). Dynamic Controls on Field-Scale Soil Nitrous Oxide Hot Spots and Hot Moments Across a Microtopographic Gradient. *Journal of Geophysical Research: Biogeosciences*, *124*(11), 3618–3634. https://doi.org/10.1029/2019JG005224

Leifeld, J., & Menichetti, L. (2018). The underappreciated potential of peatlands in global climate change mitigation strategies. *Nature Communications*, *9*. https://doi.org/10.1038/s41467-018-03406-6

Leinfelder-Miles, M. (2019). *2019 UCCE Field Corn Variety Trial Results*.

Levy, P. E., Cowan, N., van Oijen, M., Famulari, D., Drewer, J., & Skiba, U. (2017). Estimation of cumulative fluxes of nitrous oxide: uncertainty in temporal upscaling and emission factors. *European Journal of Soil Science*, *68*(4), 400–411. https://doi.org/10.1111/ejss.12432

Linquist, B., Van Groenigen, K. J., Adviento-Borbe, M. A., Pittelkow, C., & Van Kessel, C. (2012). An agronomic assessment of greenhouse gas emissions from major cereal crops. *Global Change Biology*, *18*(1), 194–209. https://doi.org/10.1111/j.1365-2486.2011.02502.x

Lintott, P. R., & Mathews, F. (2018). Basic mathematical errors may make ecological assessments unreliable. *Biodiversity and Conservation*. Springer Netherlands. https://doi.org/10.1007/s10531-017-1418-5

Liu, H., Wrage-Mönnig, N., & Lennartz, B. (2020). Rewetting strategies to reduce nitrous oxide emissions from European peatlands. *Communications Earth & Environment*, *1*(1), 17. https://doi.org/10.1038/s43247-020-00017-2

Liu, H., Zak, D., Rezanezhad, F., & Lennartz, B. (2019). Soil degradation determines release of nitrous oxide and dissolved organic carbon from peatlands. *Environmental Research Letters*, *14*(9), 094009. https://doi.org/10.1088/1748-9326/ab3947

Liu, P. C. (1994). Wavelet Spectrum Analysis and Ocean Wind Waves. In E. Foufoula-Georgiou & P. B. T.-W. A. and I. A. Kumar (Eds.), *Wavelets in Geophysics* (Vol. 4, pp. 151–166). Academic Press. https://doi.org/https://doi.org/10.1016/B978-0-08-052087-2.50012-8

Maljanen, M., Sigurdsson, B. D., Guömundsson, J., Öskarsson, H., Huttunen, J. T., & Martikainen, P. J. (2010). Greenhouse gas balances of managed peatlands in the Nordic countries present knowledge and gaps. *Biogeosciences*, *7*(9), 2711–2738. https://doi.org/10.5194/bg-7-2711-2010

Martikainen, P. J., Nykänen, H., Crill, P., & Silvola, J. (1993). Effect of a lowered water table on nitrous oxide fluxes from northern peatlands. *Nature*, *366*(6450), 51–53. https://doi.org/10.1038/366051a0

McClain, M. E., Boyer, E. W., Dent, C. L., Gergel, S. E., Grimm, N. B., Groffman, P. M., … Pinay, G. (2003). Biogeochemical Hot Spots and Hot Moments at the Interface of Terrestrial and Aquatic Ecosystems. *Ecosystems*, *6*(4), 301–312. https://doi.org/10.1007/s10021-003-0161-9

McLean, E. O. (1982). Soil pH and Lime Requirement. In *Page, A.L., Ed., Methods of Soil Analysis. Part 2. Chemical and Microbiological Properties, American Society of Agronomy, Soil Science Society of America, Madison,* (pp. 199–224).

McNicol, G., Sturtevant, C. S., Knox, S. H., Dronova, I., Baldocchi, D. D., & Silver, W. L. (2017). Effects of seasonality, transport pathway, and spatial structure on greenhouse gas fluxes in a restored wetland. *Global Change Biology*, *23*(7), 2768–2782. https://doi.org/10.1111/gcb.13580

Molodovskaya, M., Singurindy, O., Richards, B. K., Warland, J., Johnson, M. S., & Steenhuis, T. S. (2012). Temporal Variability of Nitrous Oxide from Fertilized Croplands: Hot Moment Analysis. *Soil Science Society of America Journal*, *76*(5), 1728. https://doi.org/10.2136/sssaj2012.0039

Mondal, D., & Percival, D. B. (2010). Wavelet variance analysis for gappy time series. *Annals of the Institute of Statistical Mathematics*, *62*(5), 943–966. https://doi.org/10.1007/s10463-008-0195-z

Myhre, G., Shindell, D., Bréon, F.-M., Collins, W., Fuglestvedt, J., Huang, J., … Zhang, H. (2013). Anthropogenic and Natural Radiative Forcing. *Climate Change 2013: The Physical Science Basis. Contribution of Working Group I to the Fifth Assessment Report of the Intergovernmental Panel on Climate Change*, 659–740. https://doi.org/10.1017/ CBO9781107415324.018

O'Connell, C. S., Ruan, L., & Silver, W. L. (2018). Drought drives rapid shifts in tropical rainforest soil biogeochemistry and greenhouse gas emissions. *Nature Communications*, *9*(1), 1348.

https://doi.org/10.1038/s41467-018-03352-3

Oertel, C., Matschullat, J., Zurba, K., Zimmermann, F., & Erasmi, S. (2016). Greenhouse gas emissions from soils - A review. *Chemie Der Erde - Geochemistry*, *76*(3), 327–352. https://doi.org/10.1016/j.chemer.2016.04.002

Oikawa, P. Y., Jenerette, G. D., Knox, S. H., Sturtevant, C., Verfaillie, J., Dronova, I., … Baldocchi, D. D. (2017). Evaluation of a hierarchy of models reveals importance of substrate limitation for predicting carbon dioxide and methane exchange in restored wetlands. *Journal of Geophysical Research: Biogeosciences*, *122*(1), 145–167. https://doi.org/10.1002/2016JG003438

Oktarita, S., Hergoualc'H, K., Anwar, S., & Verchot, L. V. (2017). Substantial N2O emissions from peat decomposition and N fertilization in an oil palm plantation exacerbated by hotspots. *Environmental Research Letters*, *12*(10). https://doi.org/10.1088/1748-9326/aa80f1

Pärn, J., Verhoeven, J. T. A., Butterbach-Bahl, K., Dise, N. B., Ullah, S., Aasa, A., … Mander, Ü. (2018). Nitrogen-rich organic soils under warm well-drained conditions are global nitrous oxide emission hotspots. *Nature Communications*, *9*(1), 1–8. https://doi.org/10.1038/s41467-018-03540-1

Pellerin, B., Anderson, F. E., & Bergamaschi, B. (2014). *Assessing the role of winter flooding on baseline greenhouse gas fluxes from corn fields in the Sacramento-San Joaquin Bay Delta*. *California Energy Commission*.

Petrescu, A. M. R., Lohila, A., Tuovinen, J.-P., Baldocchi, D. D., Desai, A. R., Roulet, N. T., … Cescatti, A. (2015). The uncertain climate footprint of wetlands under human pressure. *Proceedings of the National Academy of Sciences of the United States of America*, *112*(15), 4594–4599. https://doi.org/10.1073/pnas.1416267112

Reeves, S., Wang, W., Salter, B., & Halpin, N. (2016). Quantifying nitrous oxide emissions from sugarcane cropping systems: Optimum sampling time and frequency. *Atmospheric Environment*, *136*, 123–133. https://doi.org/10.1016/j.atmosenv.2016.04.008

Rochette, P., & Eriksen-Hamel, N. S. (2008). Chamber Measurements of Soil Nitrous Oxide Flux: Are Absolute Values Reliable? *Soil Science Society of America Journal*, *72*(2), 331–342. https://doi.org/10.2136/sssaj2007.0215

Rösch, A., & Schmidbauer, H. (2018). WaveletComp: Computational Wavelet Analysis. R package

version 1.1., 1–38. Retrieved from http://www.hs-stat.com/projects/WaveletComp/WaveletComp_guided_tour.pdf%0Ahttps://cran.r-project.org/package=WaveletComp

Savage, K., Phillips, R., & Davidson, E. (2014). High temporal frequency measurements of greenhouse gas emissions from soils. *Biogeosciences*, *11*(10), 2709–2720. https://doi.org/10.5194/bg-11-2709-2014

Sihi, D., Davidson, E. A., Savage, K. E., & Liang, D. (2020). Simultaneous numerical representation of soil microsite production and consumption of carbon dioxide, methane, and nitrous oxide using probability distribution functions. *Global Change Biology*, *26*(1), 200–218. https://doi.org/10.1111/gcb.14855

Soil Survey Staff. (2020). Natural Resources Conservation Service, United States Department of Agriculture. Official Soil Series Descriptions. Available online. Accessed [June/08/2020].

Sturtevant, C., Ruddell, B. L., Knox, S. H., Verfaillie, J., Matthes, J. H., Oikawa, P. Y., & Baldocchi, D. (2016). Identifying scale-emergent, nonlinear, asynchronous processes of wetland methane exchange. *Journal of Geophysical Research: Biogeosciences*, *121*(1), 188–204. https://doi.org/10.1002/2015JG003054

Teh, Y. A., Silver, W. L., Sonnentag, O., Detto, M., Kelly, M., & Baldocchi, D. D. (2011). Large Greenhouse Gas Emissions from a Temperate Peatland Pasture. *Ecosystems*, *14*(2), 311–325. https://doi.org/10.1007/s10021-011-9411-4

Tiemeyer, B., Albiac Borraz, E., Augustin, J., Bechtold, M., Beetz, S., Beyer, C., … Zeitz, J. (2016). High emissions of greenhouse gases from grasslands on peat and other organic soils. *Global Change Biology*, *22*(12), 4134–4149. https://doi.org/10.1111/gcb.13303

Veber, G., Kull, A., Villa, J. A., Maddison, M., Paal, J., Oja, T., … Mander, Ü. (2017). Greenhouse gas emissions in natural and managed peatlands of America: Case studies along a latitudinal gradient. *Ecological Engineering*. https://doi.org/10.1016/j.ecoleng.2017.06.068

Verhoeven, J. T. A., & Setter, T. L. (2010). Agricultural use of wetlands: Opportunities and limitations. *Annals of Botany*, *105*(1), 155–163. https://doi.org/10.1093/aob/mcp172

Wiggins, B. C. (2000). Detecting and Dealing with Outliers in Univariate and Multivariate Contexts. *Annual Meeting of the Mid-South Educational Research Association*.

Windham-Myers, L., Bergamaschi, B., Anderson, F., Knox, S., Miller, R., & Fujii, R. (2018). Potential for negative emissions of greenhouse gases (CO2, CH4 and N2O) through coastal peatland re-establishment: Novel insights from high frequency flux data at meter and kilometer scales. *Environmental Research Letters*, *13*(4). https://doi.org/10.1088/1748-9326/aaae74

Wood, T. E., Detto, M., & Silver, W. L. (2013). Sensitivity of soil respiration to variability in soil moisture and temperature in a humid tropical forest. *PLoS ONE*, *8*(12). https://doi.org/10.1371/journal.pone.0080965

Yang, W. H., & Liptzin, D. (2015). High potential for iron reduction in upland soils. *Ecology*, *96*(7), 2015–2020. https://doi.org/10.1890/14-2097.1

Yang, W. H., Weber, K. A., & Silver, W. L. (2012). Nitrogen loss from soil through anaerobic ammonium oxidation coupled to iron reduction. https://doi.org/10.1038/ngeo1530

9 | Tables

Table 1. Mean (± standard error) annual N_2O and CH_4 fluxes by site year (July 1 to June 30), number of measurements, number of outlier measurements, outlier mean (± standard error) N_2O and CH_4 fluxes, mean fluxes (± standard error) without outliers included, % of the outlier contribution to total mean flux, and N_2O and CH_4 % of ecosystem GWP. Outliers were calculated separately for each year and in aggregate for the total dataset (All years).

Site Year	Mean ($g\ N_2O\ m^{-2}\ y^{-1}$)	Flux (n)	Hot moment flux (n)	Hot moment mean ($mg\ N_2O\ m^{-2}\ d^{-1}$)	Mean no hot moments ($g\ N_2O\ m^{-2}\ y^{-1}$)	Hot moment % change in mean flux	N_2O % GWP ($g\ CO_2e\ m^{-2}\ y^{-1}$)
1 (2017-2018)	3.52 ± 0.11	22,247	294	321.9 ± 8.0	2.00 ± 0.06	+76.3%	26.3%
2 (2018-	6.52 ± 0.25	23,196	147	896.4 ± 65.5	4.44 ± 0.10	+46.0%	35.0%

2019)							
3 (2019-2020)	2.35 ± 0.04	24,934	374	123.8 ± 2.0	1.69 ± 0.01	+38.5%	15.5%
All years	4.08 ± 0.10	70,377	468	535.5 ± 23.9	2.80 ± 0.04	+45.6%	26.0%

Site Year	Mean (mg CH_4 m^{-2} y^{-1})	Flux (n)	Hot moment flux (n)	Hot moment mean (mg CH_4 m^{-2} d^{-1})	Mean no hot moments (mg CH_4 m^{-2} y^{-1})	Hot moment % change in mean flux	CH_4 % GWP (g CO_2e m^{-2} y^{-1})
1 (2017-2018)	-111.0 ± 5.0	22,255	110	-44.4 ± 4.1	-31.8 ± 0.01	-249.2%	-0.13%
2 (2018-2019)	2220.1 ± 519.7	23,358	13	6235.2 ± 1953.3	958.7 ± 0.18	+132.1%	1.9%
3 (2019-2020)	171.6 ± 25.2	24,941	189	78.9 ± 5.7	-44.40 ± 0.02	+486.4%	0.18%
All years	761.4 ± 171.6	70,554	26	3293.8 ± 814.6	319 ± 0.08	+139.7%	0.7%

10 | Figure Captions

Figure 1. Daily mean greenhouse gas fluxes (± standard error) for (a) CO_2 (g CO_2 m^{-2} d^{-1}), (b) CH_4 (mg CH_4 m^{-2} d^{-1}), and (c) N_2O (mg N_2O m^{-2} d^{-1}). Black circles are daily mean flux measurements (mean n = 81 fluxes per day).

Figure 2. Daily mean (± standard error) (a) N_2O fluxes, (b) soil NO_3^- concentrations, (c) daily mean soil moisture, and (d) daily mean soil O_2 concentrations over the measurement period. Soil NO_3^-

measurements (0-10 cm depth) were conducted weekly from May 2018-May 2019. For (c) soil O_2 concentrations and (d) soil moisture, daily average values by soil depth are labeled as squares (10 cm), open circles (30 cm), and triangles (50 cm). Flooding and fertilization events are labeled with dashed and dotted lines, respectively. Gaps represent missing data (see Methods).

Figure 3. Daily mean (± standard error) values of (a) CH_4 fluxes, (b) soil NH_4^+, (c) soil moisture, and (d) soil O_2 over the measurement period across 10 cm (squares), 30 cm (open circles), and 50 cm (triangles) depths. Soil NH_4^+ measurements were conducted weekly at 0-10 cm depth from May 2018 to May 2019. Flooding and fertilization events are labeled with dashed and dotted lines, respectively. Gaps between data points in (a), (c), and (d) correspond to missing data (see Methods).

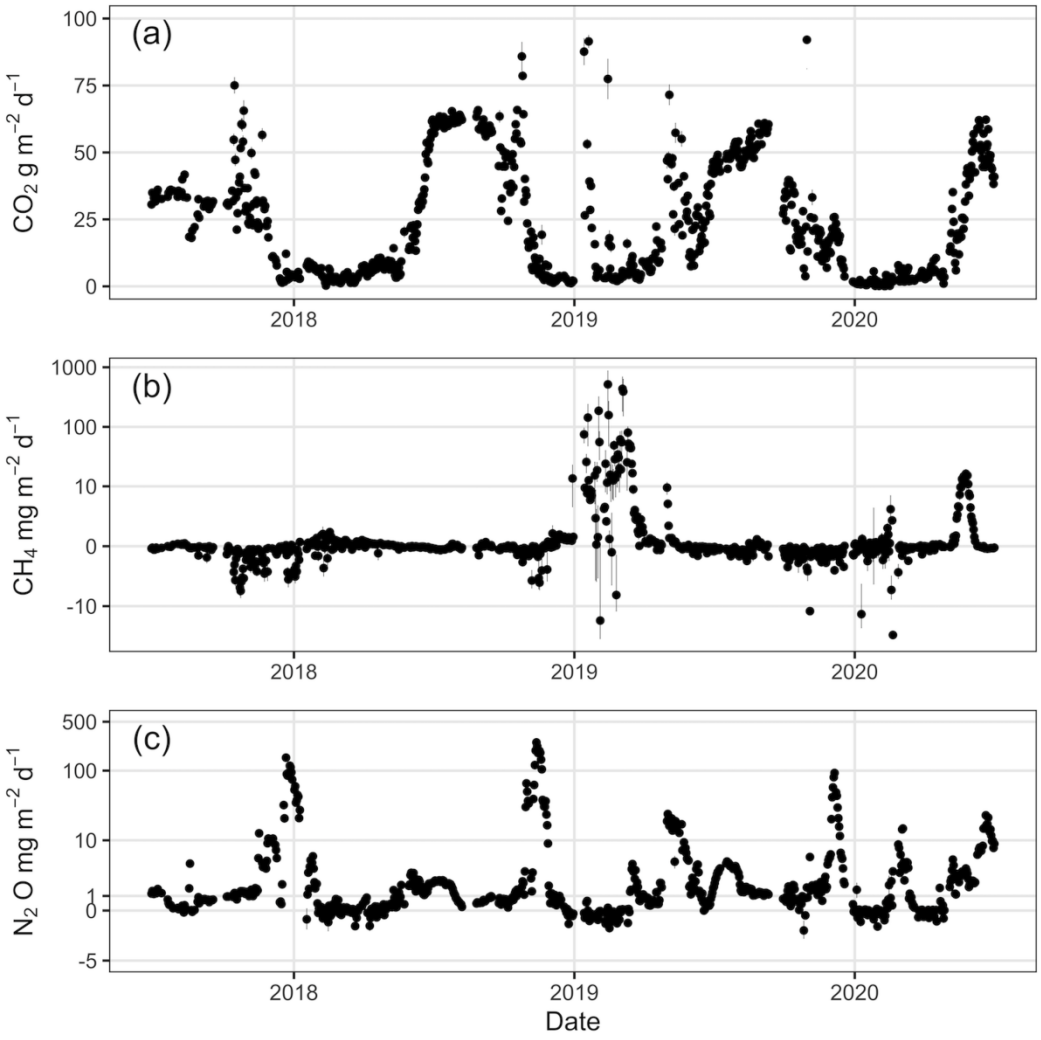

gcb_15802_f1.png

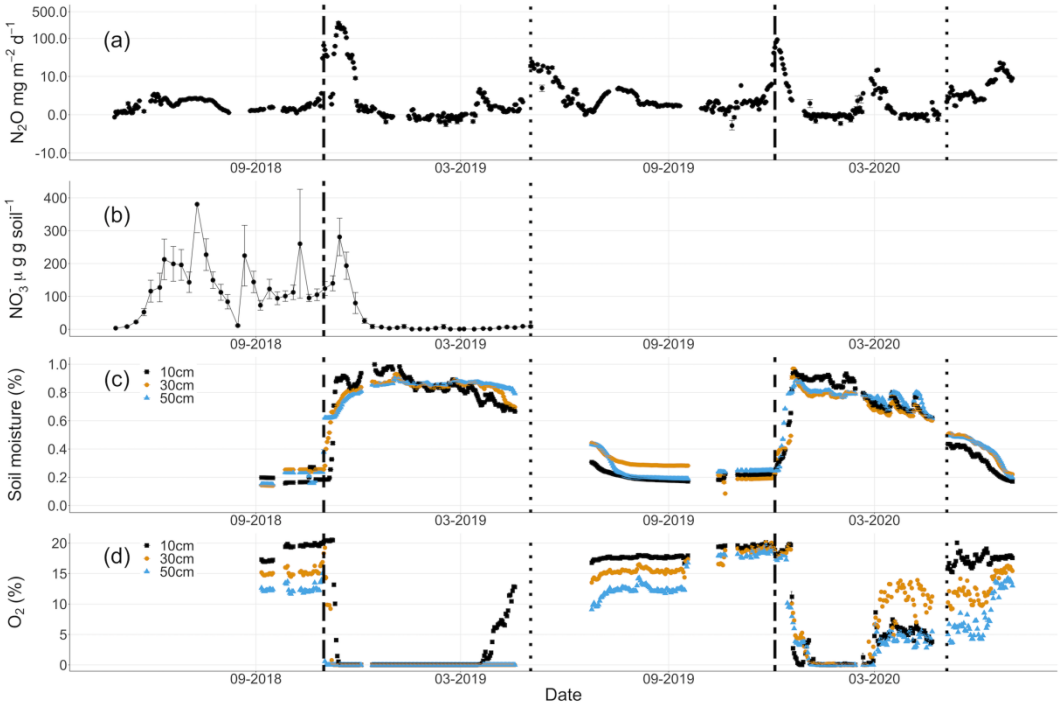

gcb_15802_f2.png

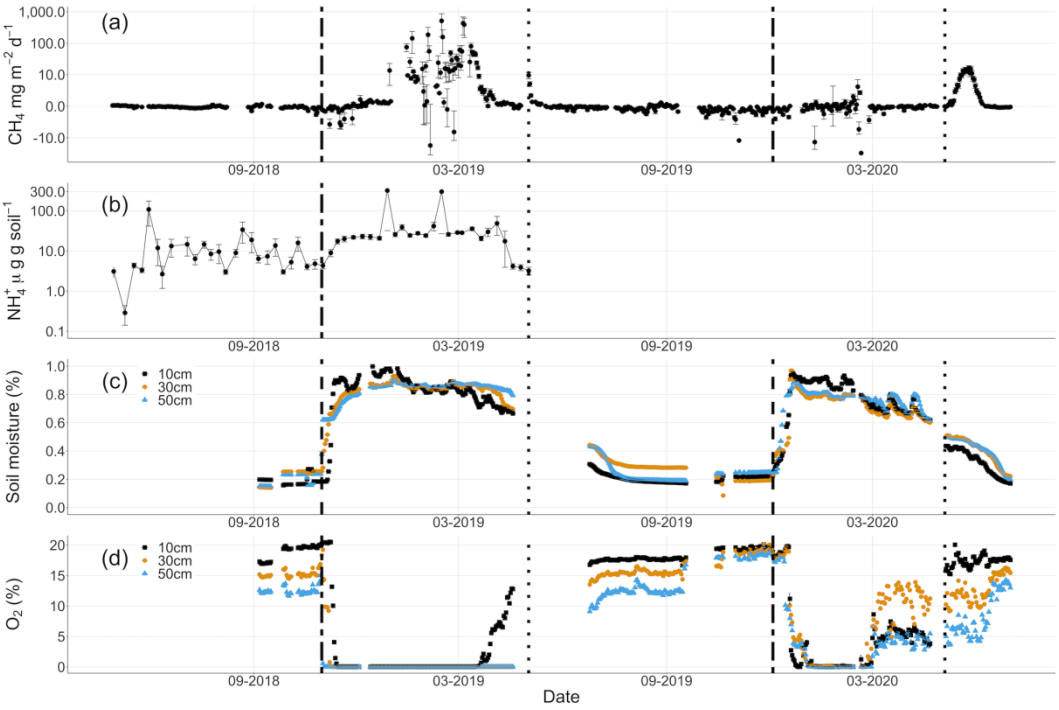

gcb_15802_f3.png